cis-[$PtBr_2\{PPh_2$(4-catechol)$\}_2$]: synthesis, crystal structure, and computational modelling of its binding to nanocrystalline TiO_2

Nigel T. Lucas,*† Andrew M. McDonagh,‡ Ian G. Dance, Stephen B. Colbran and Donald C. Craig

Received 20th September 2005, Accepted 12th December 2005
First published as an Advance Article on the web 6th January 2006
DOI: 10.1039/b513354h

The complex *cis*-[$PtBr_2\{PPh_2$(4-catechol)$\}_2$] **1** has been synthesized by cleavage of the four methyl groups from *cis*-[$PtCl_2\{PPh_2$(4-veratrole)$\}_2$] using BBr_3, followed by work-up in the presence of excess bromide. An X-ray crystal structure of **1**·$(ethanol)_2$ confirms that the two catechol rings are adjacent to each other and approximately parallel, and therefore well structured to act as double bidentate ligands for adjacent metal atoms on the surface of a nanocrystal. The crystal packing of **1**·$(ethanol)_2$ involves intermolecular hydrogen-bonding interactions and a parallel fourfold phenyl embrace between PPh_2 moieties. Density functional calculations have demonstrated that conformational variability of the aryl rings in *cis*-[$PtBr_2\{PPh_2$(4-catechol)$\}_2$] is energetically feasible, and two conformations of *cis*-[$PtBr_2\{PPh_2$(4-catechol)$\}_2$] as a complex ligand for Ti atoms on the various surfaces of the anatase and rutile structures of TiO_2 have been assessed for geometrical commensurability. Three structural models for adsorbates of *cis*-[$PtBr_2\{PPh_2$(4-catechol)$\}_2$] on TiO_2 are developed for anatase (110), anatase (101), and rutile (001).

Introduction

Immobilization of metal complexes on metal oxide supports is attracting continuing interest with applications in areas such as photovoltaics, electronic display and catalysis.[1] The immobilization of such functional complexes is usually achieved though the use of bi-functional ligands that bind the metal at one site and the oxide surface at another site. The catechol-phosphine ligand L1 (Scheme 1), first described by Raymond and co-workers,[2] has the potential to bind to soft metals through the phosphine atom, and to hard metals through the chelating catecholate group. We have previously described the synthesis of metal complexes [$PdBr_2(L1)_2$] and [$W(CO)_5$L1] and the strong adsorption of these complexes onto nanocrystalline TiO_2.[3] [$PdBr_2(L1)_2$] on TiO_2 was shown to catalyse the Sonogashira coupling of phenylacetylene and 4-iodonitrobenzene.

We present here the synthesis and crystal structure of the related platinum complex [$PtBr_2(L1)_2$] (**1**) together with a molecular modelling analysis of its adsorption on surfaces of the anatase and rutile forms of TiO_2.

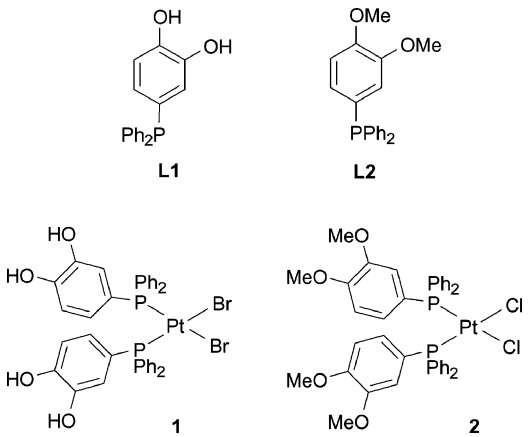

Scheme 1

Experimental

General

Reactions were carried out under an atmosphere of nitrogen using standard Schlenk techniques. All solvents were analytical grade (AR). Dichloromethane was dried and distilled over CaH_2 under a dinitrogen atmosphere. Acetone, diethyl ether, and petroleum spirit were used without drying but were purged with nitrogen prior to use. Boron tribromide (Aldrich) was used as received. Literature procedures were used to prepare [$PtCl_2(NCPh)_2$][4] and 4-(diphenylphosphino)veratrole.[2] ^{1}H and ^{31}P NMR solution spectra were recorded in $CDCl_3$ (Cambridge Isotope Laboratories or Aldrich) or d_6-acetone (Aldrich) using a Bruker Avance 300 spectrometer (at 300 MHz for ^{1}H, 121 MHz for ^{31}P). The ^{1}H NMR spectra were referenced internally to residual non-perdeuterated solvent and ^{31}P spectra to 85% H_3PO_4.

Synthesis of [$PtCl_2\{PPh_2$(4-veratrole)$\}_2$] (2). A solution of [$PtCl_2(NCPh)_2$] (604 mg, 1.28 mmol) in dichloromethane (10 mL) was added to a solution of 4-(diphenylphosphino)veratrole (L2) (870 mg, 2.70 mmol) in dichloromethane (15 mL) at room temperature with no colour change observed. The resulting clear pale-yellow solution was stirred for 2 h, the volume reduced to *ca.* 5 mL and methanol added dropwise to give a pale-yellow precipitate. The solution was cooled in ice and the precipitate

School of Chemical Sciences, The University of New South Wales, Sydney, NSW, 2052, Australia. E-mail: n.lucas@chem.usyd.edu.au
† Present address: School of Chemistry, The University of Sydney, NSW 2006, Australia.
‡ Present address: Department of Chemistry, Materials and Forensics, University of Technology Sydney, Sydney NSW 2007, Australia.

collected on a sintered glass funnel, washed with methanol and dried at the pump. Slow diffusion of diethyl ether into a dichloromethane solution (*ca.* 4 mL) of the crude material yielded white to pale-yellow crystals of $[PtCl_2\{PPh_2(4\text{-veratrole})\}_2]$ **2** (524 mg, 45%) from which the solution was decanted and residue dried *in vacuo*. ^{1}H NMR ($CDCl_3$): δ 7.61–7.51 (m, 8H, Ph), 7.37–7.29 (m, 4H, Ph), 7.24–7.16 (m, 8H, Ph), 6.98 (dd, 12 Hz, 2 Hz, 2H, C_6H_3), 6.91–6.83 (m, 2H, C_6H_3), 6.58 (dd, 8 Hz, 2 Hz, 2H, C_6H_3), 3.84 (s, 6H, Me), 3.52 (s, 6H, Me). ^{31}P NMR ($CDCl_3$): 16.3 (s, $^1J_{P,Pt} = 3660$ Hz).

Synthesis of $[PtBr_2\{PPh_2(4\text{-catechol})\}_2]$ (1). A solution of $[PtCl_2\{PPh_2(4\text{-veratrole})\}_2]$ (330 g, 0.36 mmol) in dichloromethane (20 mL) was cooled to −80 °C and BBr_3 (0.18 mL, 1.9 mmol) added dropwise and the stirred mixture was allowed to warm to room temperature over 3 h. The volatile materials were removed *in vacuo*, *ca.* 2 mL of methanol added with stirring to quench any remaining BBr_3, and the mixture again taken to dryness *in vacuo*. The crude material was dissolved in acetone (20 mL) and KBr (1.98 g, 16.6 mmol) was added and the suspension stirred vigorously for 20 h. The mixture was transferred to a separating funnel, dichloromethane (50 mL), water (100 mL) and two drops of conc. HBr were added. The organic layer was extracted, dried over Na_2SO_4, filtered and the solvent removed *in vacuo* to give an oily white solid. The crude material was triturated with petroleum spirit–acetone (9 : 1) and on standing (*ca.* 1 week) gave pale yellow crystals of $[PtBr_2\{PPh_2(4\text{-catechol})\}_2]$ **1** (205 mg, 60%). ^{1}H NMR (d_6-acetone): δ 8.32 (s, 4H, OH), 7.44–7.10 (m, 20H, Ph), 7.03 (br t, 2H, C_6H_3), 6.72 (br d, 2H, C_6H_3), 6.09 (br s, 2H, C_6H_3). ^{31}P NMR (d_6-acetone): 14.9 (s, $^1J_{P,Pt} = 3630$ Hz).

Crystallography

Crystals of **1**·(ethanol)$_2$ suitable for single-crystal X-ray analysis were produced by slow diffusion of ethanol into a solution of **1** in dichloromethane at ambient temperature. Reflection data were measured with an Enraf-Nonius CAD-4 diffractometer and were not corrected for absorption. The positions of all atoms in the asymmetric unit were determined by direct phasing (SIR92).[5] The OH and methyl hydrogen atoms were first approximately located from a difference Fourier map, then recalculated during the refinement such that O–H/C–H = 1.00 Å; all other hydrogen atoms were included in calculated positions with C–H = 1.00 Å.

Crystal data. $C_{36}H_{30}Br_2O_4P_2Pt\cdot 2(C_2H_6O)$, $M = 1035.6$, $T = 294$ K, triclinic, space group $P\bar{1}$ (no. 2), $a = 11.032(4)$, $b = 11.686(4)$, $c = 15.342(5)$ Å, $\alpha = 83.44(2)$, $\beta = 87.94(2)$, $\gamma = 87.97(2)°$, $V = 1963(1)$ Å^3, $Z = 2$, $D_c = 1.75$ g cm^{-3}, μ(Mo-Kα) = 5.751 mm^{-1}, $F(000) = 1016.0$, scan mode $\theta/2\theta$, $\theta_{max} = 23°$, 5426 intensity measurements, 4624 independent observed reflections [$I > 2\sigma(I)$], 4624 data and 237 parameters in the final refinement, $R = 0.035$, $wR = 0.043$ [$I > 2\sigma(I)$], $w = 1/[\sigma^2(F) + 0.0004F^2]$, GOF = 1.32, max./min. peak in final diff. map = 1.18/−1.74 e Å^{-3}.

CCDC reference number 280146.

For crystallographic data in CIF or other electronic format see DOI: 10.1039/b513354h

Computer modelling

Alternative conformations of **1** were investigated using density functional methods: program DMol3,[6] with functional blyp, numerical basis set dnp, and scalar relativistic corrections. The modelling of these conformations on the surfaces of anatase and rutile was done by least squares fitting of positions of the set of three or four O atoms of the complex to sets of O atoms on the surface, using the program InsightII.[7] Models for surfaces of TiO_2 were generated using CrystalMaker,[8] which was used also for the creation of published figures.

Results and discussion

Synthesis

$[PtCl_2\{PPh_2(4\text{-veratrole}\}_2]$ **2** was synthesized by the reaction of $[PtCl_2(NCPh)_2]$ with 4-(diphenylphosphino)veratrole[3] in dichloromethane at room temperature. The ^{1}H NMR spectrum shows the expected phenyl, veratrole ring, and methoxy resonances. The ^{31}P NMR spectrum contains a singlet flanked by ^{195}Pt satellites at 16.4 ppm ($^1J_{P,Pt} = 3660$ Hz) and is consistent with the *cis* geometry.[9] Treatment of **2** with boron tribromide cleaves the methyl groups from the veratrole units to give a crude (diphenylphosphino)catechol platinum complex **1**, which was purified by recrystallisation from a dichloromethane–diethyl ether mixture. This reaction is in contrast to that of $[PdCl_2\{PPh_2(4\text{-veratrole}\}_2]$ where treatment with boron tribromide cleaves the veratrole methyl groups but also decomplexes one of the phosphine ligands from the metal to afford the dimeric species $[Pd_2Br_4\{(diphenylphosphino)catechol\}_2]$ plus the (diphenylphosphino)catechol·BBr_3 adduct.[3] $[PdBr_2\{PPh_2(4\text{-catechol})\}_2]$ can be accessed *via* an alternative route that employs L1·HBr.[3] During the reaction of **2** with boron bromide, some bromide for chloride exchange occurs. For this reason, the crude reaction mixture was stirred with excess potassium bromide to form **1** with a negligibly small amount of the chloride complex present. The ^{1}H NMR spectrum of **1** shows the expected phenyl, catechol ring and hydroxy resonances while the ^{31}P NMR spectrum contains a singlet with satellites at 14.9 ppm ($^1J_{P,Pt} = 3630$ Hz), indicative of *cis* geometry.

Crystal structure of 1

The crystal structure of **1** is the first structure of a compound of the type *cis*-$[MX_2\{PPh_2(4\text{-catechol})\}_2]$ (X = halide). Complex **1** crystallizes from a dichloromethane/ethanol mixture in the space group $P\bar{1}$ with one molecule of the complex and two molecules of ethanol in the asymmetric unit. The molecular structure has a slightly distorted *cis* square planar coordination (details in Table 1), with the phosphine ligand substituents conformed such that the two catechol rings are approximately parallel.

Table 1 Coordination distances (Å) and angles (°) for **1**

Pt1–Br1	2.475(1)	Pt1–P1	2.262(2)
Pt1–Br2	2.482(1)	Pt1–P2	2.275(2)
Br1–Pt1–Br2	85.53(3)	Br2–Pt1–P1	174.92(5)
Br1–Pt1–P1	91.91(5)	Br2–Pt1–P2	86.30(5)
Br1–Pt1–P2	170.90(5)	P1–Pt1–P2	96.53(7)

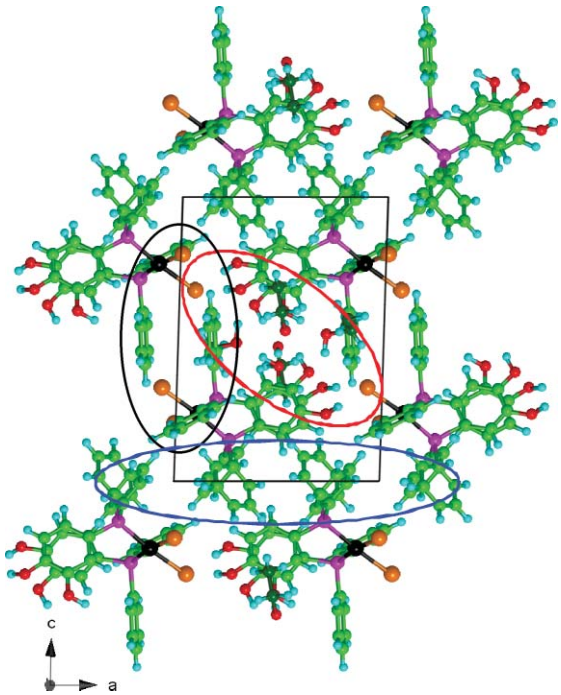

Fig. 1 The crystal packing of **1**·(ethanol)$_2$, space group $P\bar{1}$: Pt black, Br orange, P magenta, C green, O red, H cyan. The red enclosure draws attention to the segregation of hydroxyl groups from the catechol groups and the ethanol molecules (C atoms dark green). The black enclosure outlines an intermolecular (OFF)(EF)$_2$ embrace (P4PE) motif (see text), and the region enclosed in blue contains sequences of Ph_2P moieties, between which there are no EF (edge-to-face) or OFF (offset-face-to-face) motifs.

Fig. 1 shows the conformation of the complex, its packing in the crystal, and the main intermolecular domains. The two catechol rings in each molecule are approximately parallel with an average separation of 3.30 Å, and rotated so that the catechol functions are staggered. This arrangement of rings is analogous to the offset-face-to-face (OFF) arrangement of phenyl rings that commonly occurs within and between molecules. Two other related complexes, *cis*-[$PtCl_2(PPh_3)_2$][10] and *cis*-[$PtCl_2\{PPh_2(C_6H_4$-3-$CO_2H)\}_2$],[10] have similar intra-complex inter-ligand OFF interactions between phenyl groups, with inter-ring separations of 3.36 and 3.30 Å respectively.

The hydrophilic hydroxyl domain of **1**·(ethanol)$_2$ (red enclosure in Fig. 1) is shown in detail in Fig. 2. Chains of hydrogen bonds O–H···O–H···O–H···O–H···O link catechol groups and ethanol OH groups, without intramolecular hydrogen bonds between catechol groups. There are also catechol O–H···Br hydrogen bonds. Geometrical details are in Table 2.

The crystal packing of **1**·(ethanol)$_2$ contains one inter-complex embrace motif between PPh_2 moieties (black enclosure, Fig. 1),

Table 2 Selected hydrogen bonding distances (H···A) for **1**·(ethanol)$_2$ (Å) (O–H bond lengths normalized to 1.00 Å)[a]

O3–H1O3···O1Et2	1.70	O1Et1–H1O1Et1···O2	1.87
O1Et2–H1O1Et2···O1^{i}	1.99	O2–H1O2^{ii}···Br2	2.38
O1–H1O1^{i}···O1Et1	1.62	O4–H1O4^{ii}···Br2	2.46

[a] Symmetry codes: i = 1 − x, 1 − y, 1 − z; ii = x − 1, y, z.

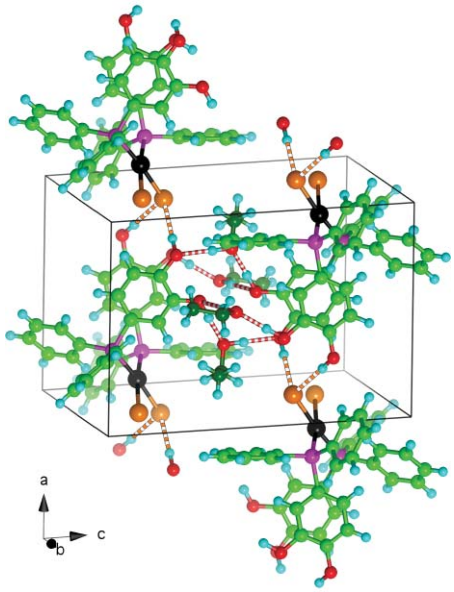

Fig. 2 The hydroxyl domain of the crystal packing of **1**·(ethanol)$_2$. There are two chains of four hydrogen bonds (red and white stripes, O–H···O–H···O–H···O–H···O) linking two molecules of **1** and four ethanol molecules (C dark green). Of the four OH groups per molecule of **1**, two are involved in these hydroxyl hydrogen bonded chains, and the other two form O–H···Br hydrogen bonds, marked as orange/white stripes.

namely the centrosymmetric parallel fourfold phenyl embrace or (OFF)(EF)$_2$ combination (OFF = offset-face-to-face, EF = edge-to-face) that is common in complexes of this type.[11]

The structure of 1 bound to TiO_2 nanoparticles

Examination of the crystal structure of **1** reveals that the two catechol rings are adjacent to each other and approximately parallel, and therefore well structured to act as double bidentate ligands for adjacent metal atoms on the surface of a nanocrystal. Thus, the structure of **1** allows us to evaluate how it could bind to faces of TiO_2 nanocrystals. Commonly available TiO_2 nanocrystals (*e.g.* Degussa P25) often contain a mixture of anatase and rutile phases[12] and so both TiO_2 structures have been considered. The extensive research on the structures of TiO_2 surfaces has been comprehensively reviewed.[13]

In our previous experiments[3] a small excess of the base NEt_3 was used and so the two catechol groups will be significantly deprotonated when coordinated to Ti. The four donor O atoms of the complex are not coplanar, which is a structural restriction because the O atoms that they would replace on TiO_2 crystallographic faces are coplanar. Therefore we first investigated whether the conformation of **1** that occurs in the crystal could change on surface binding such that the four catecholate O atoms become coplanar. Alternative conformations were generated by rotation around the Pt–P and P–C bonds, and then optimised by density functional calculations, as was the molecular structure in the crystal. The most favourable alternative conformation **1b** is shown in Fig. 3, in comparison with the conformation **1a** in the crystal. Conformer **1b**, which is 8 kcal mol^{-1} less stable, has the four catechol O atoms within 0.2 Å of their mean plane. Both **1a** and **1b** were considered in modelling the binding to TiO_2 surfaces,

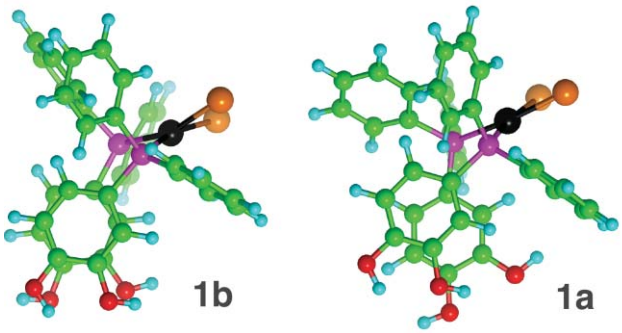

Fig. 3 An alternative conformation **1b** of *cis*-[$PtBr_2\{PPh_2$(4-catechol)$\}_2$], in comparison with the crystal conformation **1a** (both optimised by density functional methods). Both are viewed normal to the parallel catechol rings. In **1b** some phenyl ring conformations are different, to maintain appropriate intramolecular non-bonded interactions. The separations of the parallel catechol rings are 3.56 Å (**1a**), 3.54 Å (**1b**).

which was done by comparing the geometry of their arrays of four O atoms with the geometries of all sets of four O atoms on the various surfaces of anatase and rutile. This analytical procedure permits assessment of the commensurability of **1a** and **1b** with chelation of Ti at any surface of TiO_2. We also recognised the possibility that one or two of the catechol OH groups might form a hydrogen bond with O or OH within the TiO_2 surface, instead of chelating Ti.

For anatase (tetragonal, space group $I4_2/amd$) the (101) and (100)(010) surfaces are observed, with some (001): the (101) face is the most thermodynamically stable. For rutile (tetragonal, space group $P4_2/mmm$) the observed faces are (110) (most stable), (101)(011) and (001). Each of these surfaces was investigated, together with anatase (110), with **1a** and **1b**.

Most combinations showed geometrical incompatibility between the O atoms of the complex and O atom positions completing the coordination of surface Ti. Two good fits for three of the O atoms of conformer **1a** occur, with anatase (110) and rutile (001). In these the fourth O of the ligand is not bound to the surface. Fig. 4(a) shows detail for **1a** bound to a section of the anatase (110) surface, which, when neutral, contains four-coordinate Ti atoms. One catechol chelates one Ti, while the other catechol completes five-coordination of a nearby Ti. An arrangement of three close molecules of **1a** bound to the anatase (110) surface is illustrated in Fig. 4(b).

Titanium atoms on the rutile (001) surface also have two vacant coordination positions, and are arranged such that the complex **1a** can chelate as a bidentate plus monodentate ligand. Details of the coordination are shown in Fig. 5(a), and an arrangement of four molecules of **1a** on the surface is shown in Fig. 5(b).

Since anatase is the predominant component of the TiO_2 material used in our experiments, and the (101)(011)(10$\bar{1}$)(01$\bar{1}$) surfaces of anatase are most stable and prevalent in single crystals,[13] this surface type needs to be carefully considered as the domain for binding of *cis*-[$PtBr_2\{PPh_2$(4-catechol)$\}_2$]. The neutral form of this surface has a sawtooth structure with two-coordinate O atoms on the ridges and five-coordinate Ti atoms on the slopes (see Fig. 6(a)), with surface reconstruction involving shifts of $\leq$0.2 Å.[13] The array of positions for O atoms ligating this surface is essentially rectangular, which means that **1b** is better able

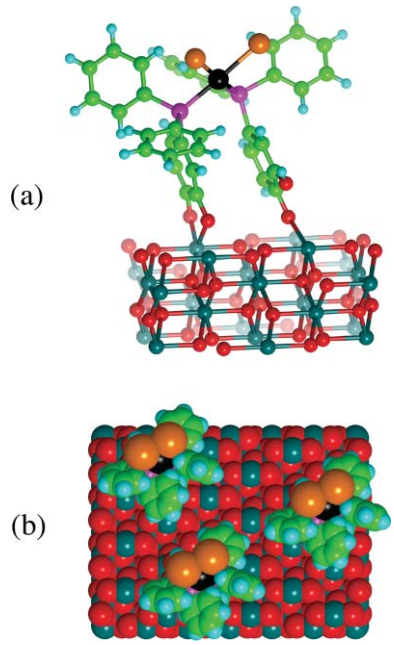

Fig. 4 Representations of **1a** bound to the anatase (110) surface. (a) Detail of the bidentate plus monodentate chelation of two adjacent Ti atoms. (b) Space-filling representation of three bound molecules of **1a**, viewed normal to the face.

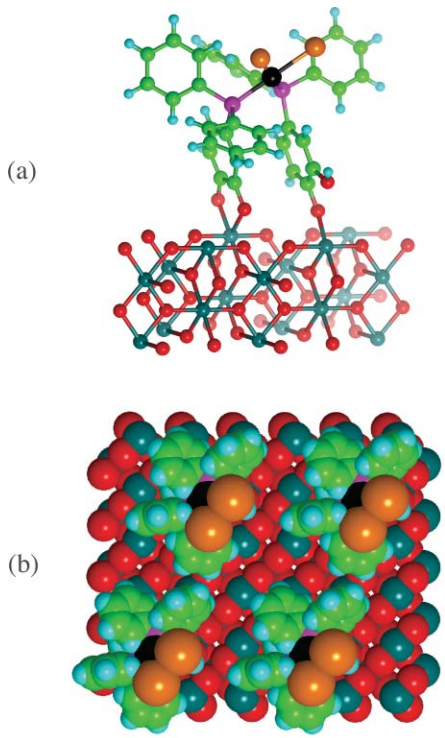

Fig. 5 (a) Detail of **1a** bound to the (001) surface of rutile. (b) Space-filling representation of one of the possible arrangements of four molecules of **1a** bound to rutile (001), viewed normal to the face.

to bind to it. Two possibilities were identified. One has only one deprotonated O of each catechol ligand coordinated to Ti, with the other OH group hydrogen bonded to O atoms on the ridges of the surface: this structure is disfavoured by the stereochemistry

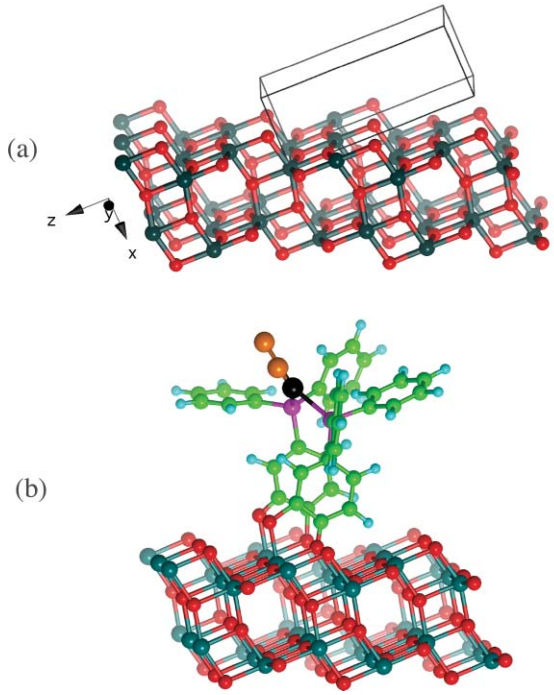

Fig. 6 (a) The sawtooth structure of anatase (101), with five-coordinate Ti on the slopes. The separation of Ti atoms in the [010] direction is 3.79 Å, which matches the separation of catechol rings in **1a** and **1b**. (b) The favourable double-bidentate chelation of Ti in anatase (101) by **1b**.

at the ligating catecholate O atom, which is too close to linear. The other possibility has **1b** functioning as a double-bidentate ligand, with one catecholate O atom of each catechol occupying the sixth coordination position of Ti, and the other catecholate O substituting for a ridge O atom of the surface. This coordination mode is illustrated in Fig. 6(b).

Discussion

Density functional calculations have demonstrated the conformational variability of the aryl rings in *cis*-[$PtBr_2${PPh_2(4-catechol)}$_2$], such that the separation of the catechol rings can increase by up 0.4 Å, and the catechol rings can rotate from staggered towards eclipsed conformation, thereby adjusting the presentation of the four catechol O atoms to the surface metal atoms. In the crystal conformation **1a** the four O atoms of the complex-ligand are not coplanar, while in conformation **1b** they are near coplanar. The calculated energy difference of 8 kcal mol^{-1} between **1a** and the energetically disfavoured (but conformationally favoured) **1b** is relatively small and so would be no impediment to adsorption.

The structures of TiO_2 surfaces are relatively rigid geometrically, with reconstructive atom shifts of order 0.2 Å.[13] Using the criteria of (a) geometrical compatibility between complex-ligand O atom sets and O atom sets that complete the coordination of surface Ti atoms in rutile or anatase, and (b) an absence of other steric conflicts between ligand and surface atoms, we have identified just three possible binding modes. Two of these involve the complex-ligand in its crystal conformation, functioning as a bidentate plus monodentate chelator of surface Ti at the anatase (110) or rutile (001) surfaces. The third involves the alternative ligand conformation **1b** functioning as a double bidentate chelator of Ti atoms at the anatase (101) surface. Other commonly occurring surfaces of anatase and rutile are incommensurate with the ligand. Because the TiO_2 particles used in our experiments on this system have dimensions of order 25 nm, edge-binding is expected to be minor relative to face-binding, and has not been evaluated.

Neutral balance of surface charge occurs in the model for **1** doubly chelating anatase (101) (Fig. 6(b)), because each catecholate^{2-} replaces one surface O^{2-}. The two other models involving **1** add 3− per ligand, to be compensated by protonation of three surface O^{2-}.[14] Indication of the surface coverage is provided in Figs. 4(b) and 5(b): the packing of molecules of *cis*-[$PtBr_2${PPh_2(4-catechol)}$_2$] on the surface depends on the surface structure, but each molecule covers at least nine surface Ti atoms. It is not evident from the modelling that phenyl–phenyl interactions between adjacent *cis*-[$PtBr_2${PPh_2(4-catechol)}$_2$] complexes, as occur in the crystal, are likely to influence the adsorption of *cis*-[$PtBr_2${PPh_2(4-catechol)}$_2$] on TiO_2 surfaces. In all three models the $PtBr_2$ points away from the surface and should be accessible for further reaction (*e.g.* catalysis) to take place.

Chelating ligands similar to but more flexible than *cis*-[$PtBr_2${PPh_2(4-catechol)}$_2$] bound to TiO_2 surfaces have been investigated experimentally and theoretically, including phosphonic acid ($HP(OH)_2$) on anatase (101),[15] bi-isonicotinic acid (2,2′-bipyridine-4,4′-dicarboxylic acid) on rutile (110),[16] and a number of carboxylic acids.[13] STM images of benzoic acid on rutile (110) provide evidence for pair-association of the phenyl rings separated by *ca.* 5.9 Å,[17] larger than the 3.3–3.7 Å separation of the catechol rings in *cis*-[$PtBr_2${PPh_2(4-catechol)}$_2$].

Acknowledgements

This research was supported by the Australian Research Council, the Australian Partnership for Advanced Computing, and The University of New South Wales.

References

1 P. F. H. Schwab, S. Diegoli, M. Biancardo and C. A. Bignozzi, *Inorg. Chem.*, 2003, **42**, 6613; C. W. Jones, M. W. McKittrick, J. V. Nguyen and K. Yu, *Top. Catal.*, 2005, **34**, 67; M. K. Nazeeruddin and M. Grätzel, in *Comprehensive Coordination Chemistry II*, ed. J. A. McCleverty and T. J. Meyer, Elsevier Ltd., Oxford, UK, 2004, vol. 9, p. 719; D. J. Cole-Hamilton, *Science*, 2003, **299**, 1702.
2 X. Sun, D. Johnson, D. Caulder, K. Raymond and E. Wong, *J. Am. Chem. Soc.*, 2001, **123**, 2752.
3 N. Lucas, J. Hook, A. McDonagh and S. Colbran, *Eur. J. Inorg. Chem.*, 2005, 496.
4 P. Braunstein and J. Bender, *Inorg. Synth.*, 1989, **26**, 341.
5 A. Altomare, M. Cascarano, C. Giacovazzo, A. Guagliardi, M. C. Burla, G. Polidori and M. Camalli, *J. Appl. Crystallogr.*, 1994, **27**, 435.
6 B. Delley, *J. Chem. Phys.*, 1990, **92**, 508; B. Delley, *J. Chem. Phys.*, 2000, **113**, 7756; DMol3, www.accelrys.com/mstudio/ms_modeling/dmol3.html, 2005.
7 InsightII, www.accelrys.com/products/insight/, 2003.
8 Crystalmaker, www.crystalmaker.co.uk, 2005.
9 J. MacDougall, J. Nelson and F. Mathey, *Inorg. Chem.*, 1982, **21**, 2145.
10 G. Anderson, H. Clark, J. Davies, G. Ferguson and M. Parvez, *J. Crystallogr. Spectrosc. Res.*, 1982, **12**, 449.
11 I. Dance and M. Scudder, *Chem. Eur. J.*, 1996, **2**, 481; M. Scudder and I. Dance, *J. Chem. Soc., Dalton Trans.*, 1998, 3155; I. Dance, *Mol. Cryst. Liq. Cryst.*, 2005, **440**, 265.

12 Suppliers product information for Aeroxide TiO2 P25, www1.sivento.com/wps/portal/p3.
13 U. Diebold, *Surf. Sci. Rep.*, 2003, **48**, 53.
14 A. Barnard, P. Zapol and L. Curtiss, *Surf. Sci.*, 2005, **582**, 173.
15 M. Nilsing, S. Lunell, P. Persson and L. Ojamäe, *Surf. Sci.*, 2005, **582**, 49.
16 F. Patthey, H. Rensmo, P. Persson, K. Westermark, L. Vayssieres, A. Stashans, Å. Petersson, P. Brühwiler, H. Siegbahn, S. Lunell and N. Mårtensson, *J. Chem. Phys.*, 1999, **110**, 5913; P. Persson, S. Lunell, P. Brühwiler, J. Schadt, S. Södergren, J. O'Shea, O. Karis, H. Siegbahn, N. Mårtensson, M. Bässler and F. Patthey, *J. Chem. Phys.*, 2000, **112**, 3945.
17 Q. Guo and E. Williams, *Surf. Sci.*, 1999, **433–435**, 322.